

PAPER • OPEN ACCESS

## U-drawing of Fortiform 1050 third generation steels. Numerical and experimental results

To cite this article: E. Saenz de Argandoña *et al* 2017 *J. Phys.: Conf. Ser.* **896** 012118

View the [article online](#) for updates and enhancements.

### Related content

- [Numerical simulation of the roll levelling of third generation fortiform 1050 steel using a nonlinear combined hardening material model](#)  
L Galdos, E Saenz de Argandoña, J Mendiguren *et al.*
- [Influence of hardening functions on earing prediction in cup drawing of AA3104 aluminum alloy sheet](#)  
H Fukumasu, T Kuwabara, H Takizawa *et al.*
- [Experimental evaluation of Bauschinger effects during tension-compression in-plane deformation of sheet materials](#)  
M Härtel, C Illgen and M F-X Wagner



**IOP | ebooks™**

Bringing you innovative digital publishing with leading voices to create your essential collection of books in STEM research.

Start exploring the collection - download the first chapter of every title for free.

# U-drawing of Fortiform 1050 third generation steels. Numerical and experimental results

E. Saenz de Argandoña<sup>1</sup>, L. Galdos<sup>1</sup>, J. Mendiguren<sup>1</sup>, I. Otero<sup>1</sup> and E. Mugarra<sup>1</sup>

<sup>1</sup>Mechanical and Manufacturing Department  
Mondragon University  
Loramendi 4, 20500 Arrasate-Mondragon, Spain

e-mail: esaenzdeargan@mondragon.edu, Web page: www.mondragon.edu

**Abstract.** Elasto–plastic behavior of the third generation Fortiform 1050 steel has been analysed using cyclic tension–compression tests. At the same time, the pseudo elastic modulus evolution with plastic strain was analysed using cyclic loading and unloading tests. From the experiments, it was found that the cyclic behavior of the steel is strongly kinematic and elastic modulus decrease with plastic strain is relevant for numerical modelling. In order to numerically analyse a U-Drawing process, strip drawing tests have been carried out at different contact pressures and Filzek model has been used to fit the experimental data and implement a pressure dependent friction law in Autoform software. Finally, numerical predictions of springback have been compared with the experimentally ones obtained using a sensorized U-Drawing tooling. Different material and contact models have been examined and most influencing parameters have been identified to model the forming of these new steels.

## 1. Introduction

During the last decades, many new grades of high-strength steel materials have been developed [1-4]. However, it is well known that the formability of steels decreases with increasing strength. This is also valid for the newly developed third generation high-strength steels as well [5]. The light weighting potential of these new commercial steels is said to be around 20% in comparison to already used Dual Phase steels. For example, the Dual Phase 780 steel has a yield strength of 480 MPa and an ultimate strength of 830 MPa. Having the same formability and comparable forming limit curve, the Fortiform 1050 steel, the material studied in this paper, has a yield strength of 760 MPa and an ultimate strength of 1100 MPa.

Besides the significant decrease in formability, the higher post-forming springback is one of the biggest technological problems when defining and developing new high strength sheet metal components. Current industrial problems when using these materials are premature cracks and excessive set-up times needed for springback compensation.

In order to achieve a good accuracy when numerically predicting the final geometry of the components two main aspects must be considered: the material model and the restraining forces due to the friction between the tool and the material. If these variables are not accurately defined the numerical predictions can be far away from the experimental results [6-7].

Concerning the material, a good definition of the hardening behavior is very important when the material suffers alternative tensile and compression cycles [8]. This is the case of deep drawing



processes when the material goes through the drawbeads and/or the die radius. Meanwhile mild steels present nearly an isotropic hardening behavior, high strength steels present a kinematic or mixed hardening behavior [9-10]. Consequently, a poor definition of the hardening behavior may result in very low accurate results of springback.

The coefficient of friction (COF) is also a significant parameter to take into account when trying to obtain accurate predictions in numerical simulation [11-12]. COF influences the restriction level of the material flow through the tools and an inaccurate definition of this parameter can induce undesirable splits, insufficient deformations and, moreover, unexpected springback phenomena. A lower COF induces lower stress-states and as a consequence higher elastic recovery [13]. Therefore, it is necessary to correctly define the COF in order to accurately predict the final geometry of the component through the numerical simulation.

Among the several works published for AHSS steels, no scientific paper has been found where the above mentioned aspects have been studied for a third generation steel. For this reason and because some new third generation steel grades are currently being launched to the market by several steel makers, the current work was carried out aiming to study the Fortiform 1050 third generation steel behavior under stamping conditions. Advanced material and tribological characterization have been performed and an U-Drawing operation is numerically and experimentally studied to analyze the effect that the different numerical models have in the final springback predictions.

## 2. Material characterization

The studied material is an electrolytically galvanized third generation Fortiform 1050 steel, from Arcelor Mittal, having a thickness of 1.2 mm. Chemical composition and mechanical properties are shown in table 1.

**Table 1.** Chemical composition and mechanical properties of Fortiform 1050

C	Mn	P	S	Si	Al	N	YS (MPa)	UTS (MPa)	A%
0.2069%	2.1755%	0.0107%	0.0005%	1.4521%	0.0366%	0.0051%	775	1235	10

Besides the mechanical properties, the Lankford or anisotropy coefficients of the material have also been obtained following the ASTM E 517-00 standard and using GOM ARAMIS digital image correlation technique. The Lankford coefficients at different directions and the monotonic hardening curve are shown in figure 1a.

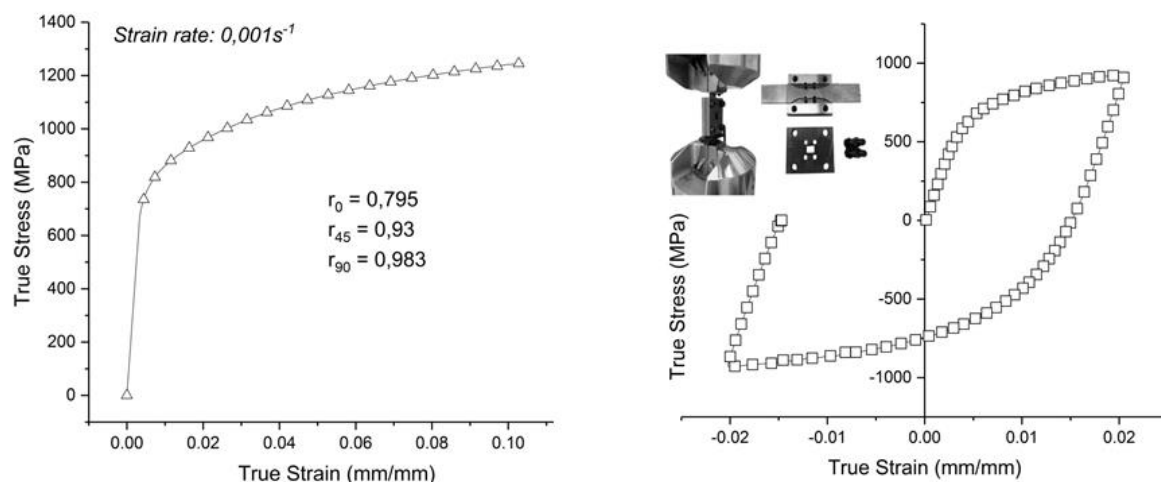


**Figure 1:** Monotonic tensile test and Lankford coefficients (a) and tensile-compression test (b) for Fortiform 1050 material

Based on these results, the monotonic behaviour of the material has been modeled using a combined Swift–Hockett/Sherby hardening model (see equation 1). The parameters of the model are as follows,  $\varepsilon_0=0.00312$ ,  $m=0.14$ ,  $C=1725$ ,  $\sigma_i=766.8$ ,  $\sigma_{sat}=1435$ ,  $a=5.91$ ,  $p=0.657$ ,  $\alpha=0.25$ .

$$\sigma = (1 - \alpha) \left\{ C(\varepsilon_{pl} + \varepsilon_0)^m \right\} + \alpha \left\{ \sigma_{sat} - (\sigma_{sat} - \sigma_i) e^{-a\varepsilon_{pl}^p} \right\} \quad (1)$$

As explained in the introduction, the cyclic hardening of the material is very important to predict the springback and therefore the final geometry of the deep drawn components. Therefore, tensile-compression tests have been carried out in order to identify the kinematic behavior of the material. A servo hydraulic MTS 810 Material Test System has been used for the experiments. Force data has been acquired through an axial load cell and strain data has been measured with small strain gauges to obtain continuous measurement.

The material has been subjected to cyclic tension compression test for hardening characterization during the experimental test. A maximum strain of +2% in tension and -2% in compression has been achieved during the tests. The experimental results and the experimental test equipment used to avoid specimen buckling are shown in figure 1b. The experimental results have been fitted to the kinematic model implemented in Autoform R7. The parameters used in the model are  $K=0.012$ ,  $\xi=0.8$ .

Finally the pseudo elastic modulus evolution with plastic strain has also been characterized for the material. For doing so, cyclic loading and unloading tests have been carried out. The evolution of the pseudo elastic modulus can be observed in figure 2.

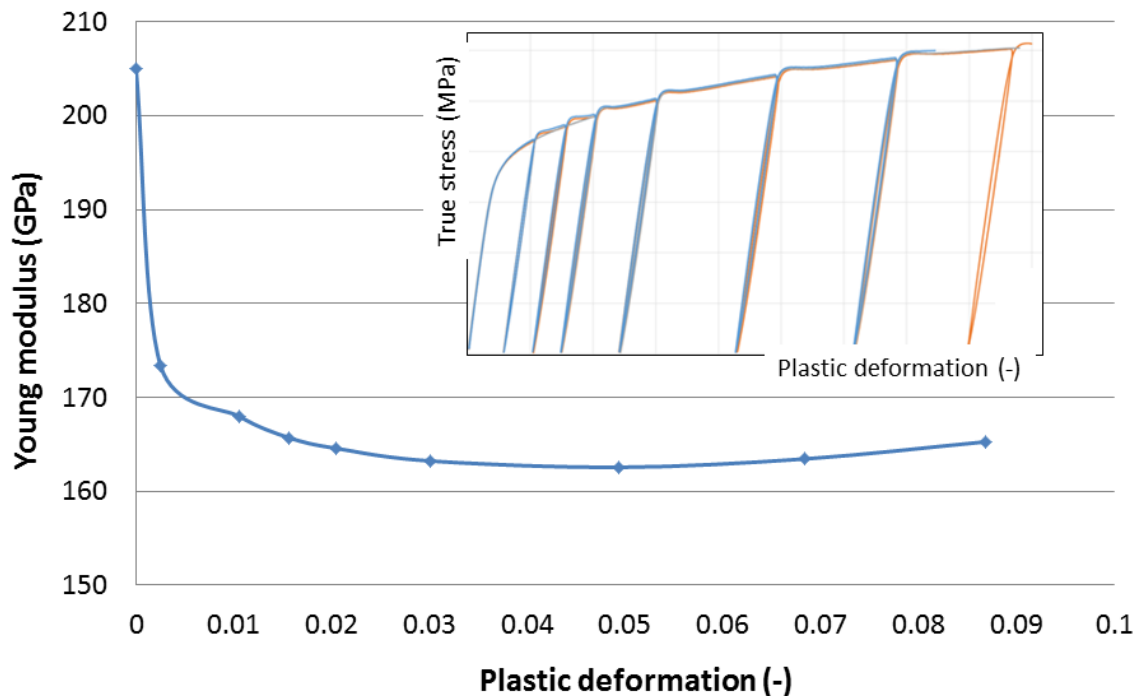


**Figure 2:** Pseudo elastic modulus evolution with plastic strain using cyclic loading and unloading tests

In the case of the pseudo elastic modulus evolution, the experimental results have also been fitted to the kinematic model implemented in Autoform R7. The parameters used in the model are  $\gamma=0.166$ ,  $\chi=4.43$ .

### 3. Tribological characterization

1.2379 tool steels hardened at 60 HRC have been used for the strip drawing tests. Same machining protocol as followed in industrial toolmakers has been used for machining and polishing the tool inserts. Roughness in longitudinal direction of tool inserts is approximately Ra0.4.

The Fortiform 1050 steel specimens are electrolytically galvanized and EDT textured. The longitudinal and transversal surface roughness of the as received material is Ra1.2 and Ra1.24 respectively.

Mild oil conditions have been used to perform the strip drawing tests and the experimental U-drawing tests. The lubricant amount of the sheets is 1.5-2.0 g/m<sup>2</sup>.

Strip drawing tests have been performed to identify the friction coefficient to be used in the numerical simulations. A range of contact pressure from 1MPa to 20MPa has been covered and a sliding velocity of 10 mm/s has been defined during the tests. The exemplary curves obtained from the normal and tangential force sensors are shown in figure 3a and the friction coefficient for the Fortiform1050 material is shown in figure 3b.

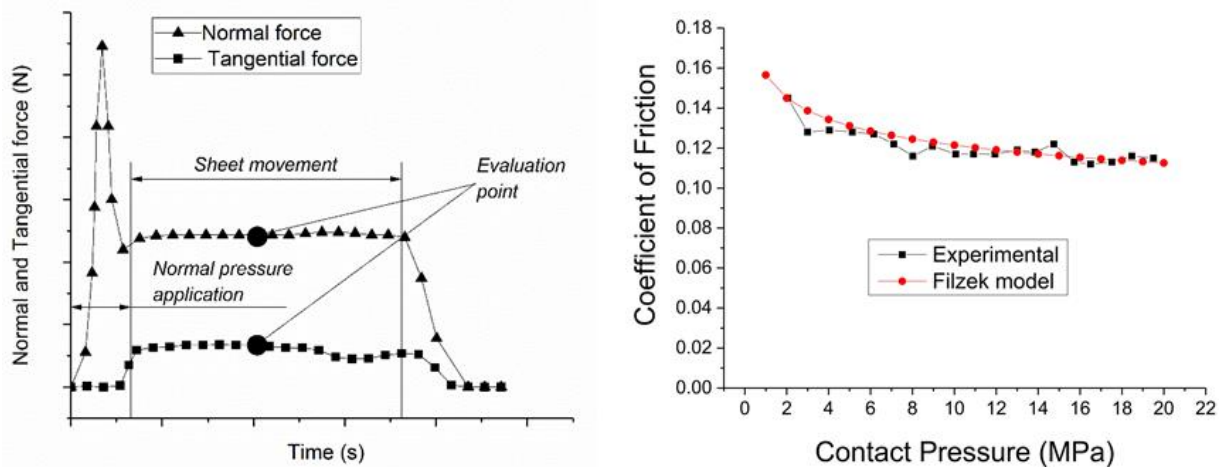


**Figure 3:** Forces measured during a strip drawing test (a) and coefficient of friction dependent on the contact pressure for Fortiform 1050 material (b)

Based on the experimental results achieved in the strip drawing tests, the parameters of the friction model proposed by Filzek (see equation 2) and implemented in Autoform have been identified. The parameters are  $\mu_0 = 0.145$ ,  $p_0 = 2$  and  $n = 0.89$ .

$$\mu = \mu_0 \left(\frac{p}{p_0}\right)^{n-1} \quad (2)$$

#### 4. U-Drawing experimental test

Experimental U-drawing tests have been performed at Mondragon University aiming to identify the best numerical models to predict springback when using third generation high strength steels. The tooling is modular and die inserts, punch inserts and drawbead inserts can be exchanged to obtain different test variables. For the present study no drawbead inserts have been used in order to avoid the influence of the drawbeads in the results. The characteristic dimensions of the configuration used for this study are summarized in table 2 while the schematic view of the tooling is shown in figure 4.

**Table 2.** Characteristic dimensions (mm) of Mondragon University's U-drawing tester

Ls	Wp	Rp	Wd	Rd	Stroke
330	100	5	106	8	70

A hydraulic press has been used to perform the drawing experiments. The drawing speed has been set to 1 mm/s, the drawing stroke has been 70 mm and 110 mm wide specimens have been used for all the tests. The blankholder force has been defined as 186kN what has given a contact pressure in the blankholder from 7.5MPa at the beginning of the drawing operation to 17.5MPa at the end of the operation due to the flow of the material.

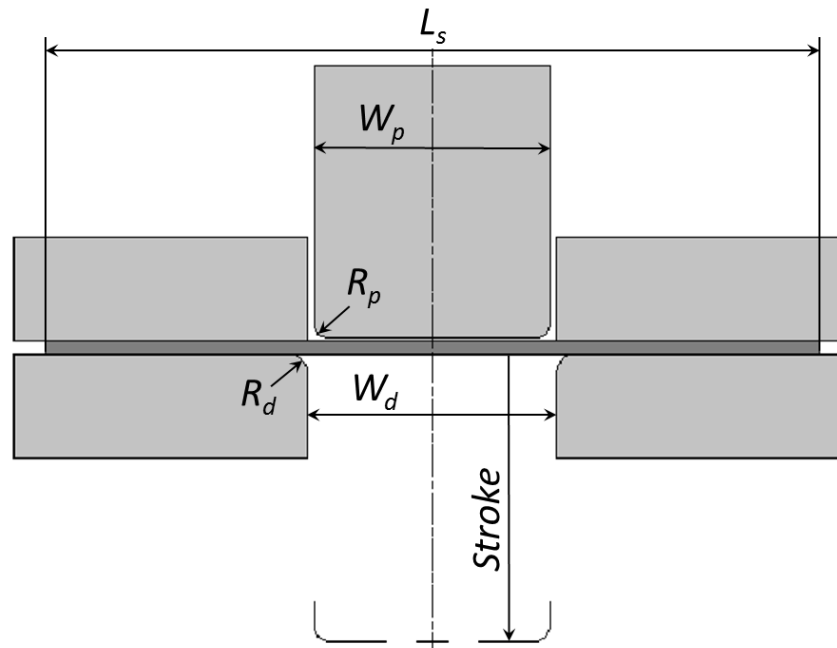


**Figure 4:** Schematic drawing of the U-Drawing tester at Mondragon University

### 5. U-Drawing test numerical simulation

Eight different numerical models have been compared in the current study using the Autoform R7 software. All simulations were defined with a sheet thickness of 1.2 mm with elastic plastic shell elements, an initial element size of 20 mm with a maximum of 4 refinement levels and 11 layers through the thickness (final validation conditions in Autoform R7). For all the models the elastic modulus has been set to 205 GPa and Hill48 yield criteria has been defined by means of the above mentioned Lankford coefficients.

Regarding the hardening behavior of the material, four different material models have been created named as Conventional, Young, Kinematic and Full. All the models have been defined using a combined Swift Hockett-Sherby hardening model. For this definition monotonic tensile test data has been used. The Conventional model does not consider any kinematic behavior of the material meanwhile the other three models do consider it.

In the case of the Full model, both the pseudo elastic modulus evolution and the kinematic behavior have been considered. For doing so, the results of the tension-compression and cyclic loading unloading tests have been fitted to the kinematic model of Autoform R7. When doing the fitting, the four parameters of the kinematic hardening model, shown in table 3, have been calculated. In the case of the Young model, only the evolution of the pseudo elastic modulus has been considered by fitting two of the parameters of the kinematic hardening model in Autoform R7 to the results achieved in the cyclic loading unloading tests. And finally, the Kinematic model only considers the kinematic evolution of the material and the other two parameters of the kinematic model in Autoform R7 have been fitted to the results achieved in the tension compression test. The coefficients of all the models are summarized in table 3.

Regarding the tribological behavior, two models have been used in the simulations. On the one hand, a constant coefficient of friction of 0.15 named as Constant has been defined. This COF value is widely used in the industry nowadays. On the other hand, a more advanced pressure dependent coefficient of friction, named as Pressure, has been used. The coefficients of both models can also be found in table 3.

**Table 3.** Numerical model input parameters

Model	Material parameters	Tribological parameters
Conventional_constant	E=205 GPa / Hill 48 ( $r_0, r_{45}, r_{90}$ )	Constant coefficient of friction $\mu = 0.15$
	Isotropic hardening – Combined S-H	
Conventional_pressure	E=205 GPa / Hill 48 ( $r_0, r_{45}, r_{90}$ )	Pressure dependent coefficient of friction $\mu_0 = 0.145$ $p_0 = 2$ $n = 0.89$
	Isotropic hardening – Combined S-H	
Young_constant	E=205 GPa / Hill 48 ( $r_0, r_{45}, r_{90}$ )	Constant coefficient of friction $\mu = 0.15$
	Isotropic hardening – Combined S-H	
	Kinematic hardening – Autoform model $K=0, \xi=0, \gamma=0.166, \chi=4.43$	
Young_pressure	E=205 GPa / Hill 48 ( $r_0, r_{45}, r_{90}$ )	Pressure dependent coefficient of friction $\mu_0 = 0.145$ $p_0 = 2$ $n = 0.89$
	Isotropic hardening – Combined S-H	
	Kinematic hardening – Autoform model $K=0, \xi=0, \gamma=0.166, \chi=4.43$	
Kinematic_constant	E=205 GPa / Hill 48 ( $r_0, r_{45}, r_{90}$ )	Constant coefficient of friction $\mu = 0.15$
	Isotropic hardening - Combined S-H	
	Kinematic hardening – Autoform model $K=0.012, \xi=0.8, \gamma=0, \chi=0$	
Kinematic_pressure	E=205 GPa / Hill 48 ( $r_0, r_{45}, r_{90}$ )	Pressure dependent coefficient of friction $\mu_0 = 0.145$ $p_0 = 2$ $n = 0.89$
	Isotropic hardening - Combined S-H	
	Kinematic hardening – Autoform model $K=0.012, \xi=0.8, \gamma=0, \chi=0$	
Full_constant	E=205 GPa / Hill 48 ( $r_0, r_{45}, r_{90}$ )	Constant coefficient of friction $\mu = 0.15$
	Isotropic hardening - Combined S-H	
	Kinematic hardening – Autoform model $K=0.012, \xi=0.8, \gamma=0.166, \chi=4.43$	
Full_pressure	E=205 GPa / Hill 48 ( $r_0, r_{45}, r_{90}$ )	Pressure dependent coefficient of friction $\mu_0 = 0.145$ $p_0 = 2$ $n = 0.89$
	Isotropic hardening - Combined S-H	
	Kinematic hardening – Autoform model $K=0.012, \xi=0.8, \gamma=0.166, \chi=4.43$	

Experimentally deep drawn specimens have been digitalized using a Mitutoyo 3D measurement machine. For geometrical accuracy comparison, GOM ATOS software and technique has been employed. The numerical and experimental results are shown in figure 5.



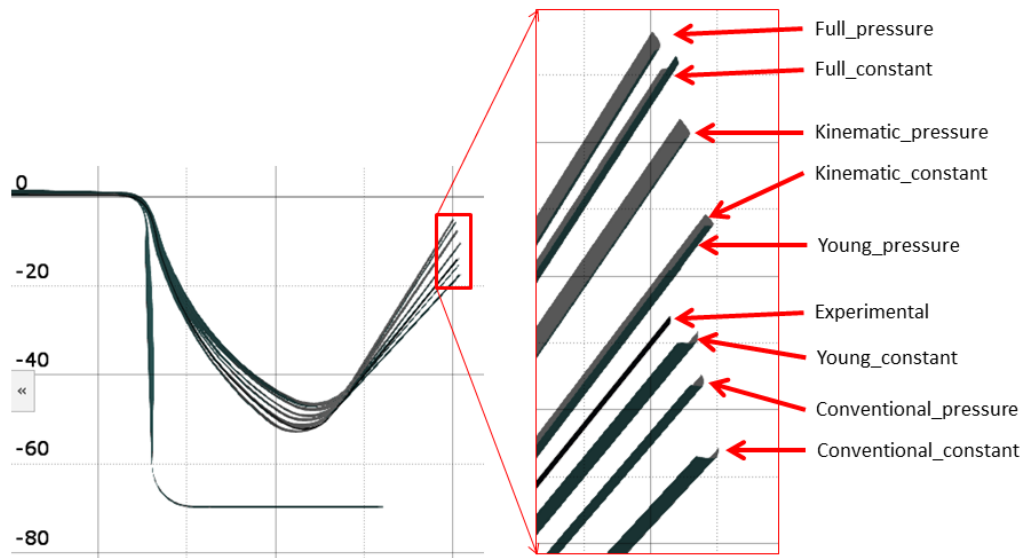


**Figure 5:** Comparison between the experimental and numerical results achieved in Autoform R7

In order to quantify the geometrical differences, the distance between the experimental component and the numerical results has also been calculated. The deviation for the different models is shown in figure 6.

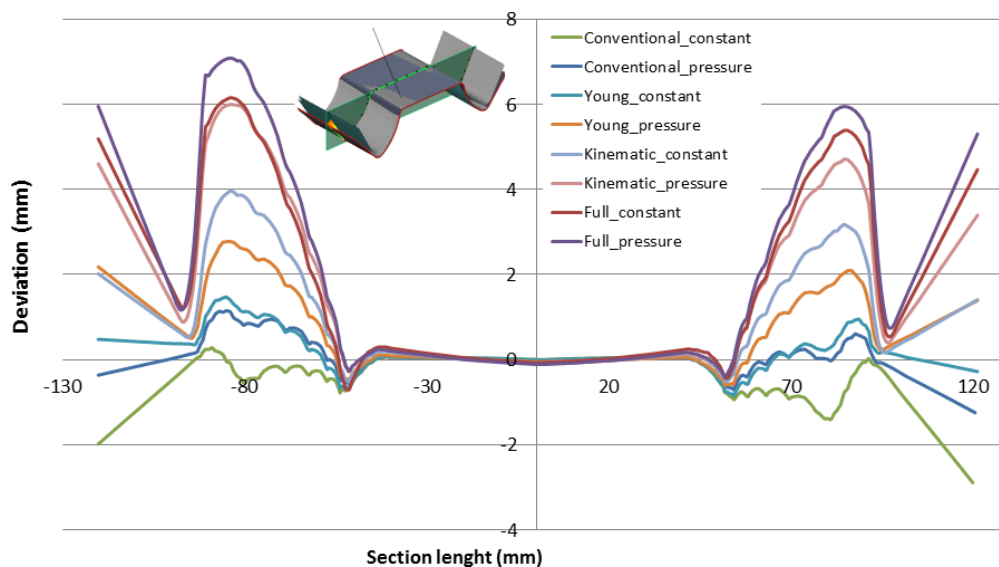


**Figure 6:** Geometrical deviation between the experimental and the numerical results

## 6. Conclusions

Many authors have recently demonstrated the importance that the hardening law, the apparent elastic modulus change and the coefficient of friction have on springback predictions. In this article the importance of using a conventional or a mixed kinematic hardening model and a constant or variable coefficient of friction has been analyzed using the Fortiform 1050 third generation steel. For the selection of the best model the final springback prediction has been used.

Regarding the material hardening model, it has been found that the conventional model, where no evolution of the pseudo elastic modulus nor the kinematic behavior are considered, gives as a result an underestimation of the springback predictions. On the other hand, if both aspects are taken into consideration, the springback predicted by the simulation is overestimated given as a result poor



springback prediction levels as well. Within that range, both the model that only considers the evolution of the pseudo elastic modulus and the model that only considers the kinematic behavior of the material give as a result intermediate springback predictions which are closer to the experimental results.

Regarding the friction between the material and the tooling, the coefficient of friction has been measured by means of strip drawing tests. At low contact pressures the coefficient of friction is about 0.145 meanwhile when increasing the contact pressure up to 20MPa the coefficient of friction decreases down to 0.12. The Filzek model is able to accurately represent the evolution of the coefficient of friction. Furthermore the introduction of the pressure dependent coefficient of friction increases the springback for all material models.

As a final conclusion, and based in the material and component geometry used at the present study, it can be stated that the material model which best predicts the final geometry of the component is the one that only considers the evolution of the pseudo elastic modulus, named as Young model at the present study. In terms of the friction model, it can be stated that the used of the pressure dependent coefficient of friction increases the springback of the component for all the analyzed material models. Therefore, engineers should take into consideration the change of the pseudo elastic modulus and the variable coefficient of friction when simulating drawing processes for third generation steels.

### Acknowledgments

The authors would like to thank the Basque and Spanish Governments for the funding of the project THIRDFORM (Elkartek funding by the Basque Government) and the project HRD: High Reliability Dies under the program RETOS with reference number RTC-2015-3643-4 and financed by Ministry of Economy and Competitiveness of the Spanish Government The collaboration and technical support in the study of the companies GESTAMP, FAGOR ARRASATE S. Coop. and MATRICI S. Coop. is also gratefully acknowledged.

### References

- [1] Fonstein, N. (2015). Advanced High Strength Sheet Steels.
- [2] Matlock, D. K., Speer, J. G., De Moor, E., & Gibbs, P. J. (2012). Recent developments in advanced high strength sheet steels for automotive applications: an overview. *Jestech*, 15(1), 1-12.
- [3] Matlock, D. K., & Speer, J. G. (2009). Third generation of AHSS: microstructure design concepts. In *Microstructure and texture in steels* (pp. 185-205). Springer London.
- [4] Speer, J. G., De Moor, E., Findley, K. O., Matlock, D. K., De Cooman, B. C., & Edmonds, D. V. (2011). Analysis of microstructure evolution in quenching and partitioning automotive sheet steel. *Metallurgical and Materials Transactions A*, 42(12), 3591-3601.
- [5] Tisza, M., & Lukács, Z. (2015). Formability Investigations of High-Strength Dual-Phase Steels. *Acta Metallurgica Sinica (English Letters)*, 28(12), 1471-1481.
- [6] Eggertsen, P. A., & Mattiasson, K. (2012). Experiences from experimental and numerical springback studies of a semi-industrial forming tool. *International journal of material forming*, 5(4), 341-359.
- [7] Hol, J. (2013). Multi-scale friction modeling for sheet metal forming. University of Twente.
- [8] Bruschi, S., Altan, T., Banabic, D., Bariani, P. F., Brosius, A., Cao, J., ... & Tekkaya, A. E. (2014). Testing and modelling of material behaviour and formability in sheet metal forming. *CIRP Annals-Manufacturing Technology*, 63(2), 727-749.
- [9] Silvestre, E., Mendiguren, J., Galdos, L., & de Argandoña, E. S. (2015). Comparison of the hardening behaviour of different steel families: From mild and stainless steel to advanced high strength steels. *International journal of mechanical sciences*, 101, 10-20.
- [10] Weiss, M., Kupke, A., Manach, P. Y., Galdos, L., & Hodgson, P. D. (2015). On the Bauschinger effect in dual phase steel at high levels of strain. *Materials Science and Engineering: A*, 643, 127-136.
- [11] Chen, P., & Koç, M. (2007). Simulation of springback variation in forming of advanced high strength steels. *Journal of Materials Processing Technology*, 190(1), 189-198.
- [12] Gil, I., Mendiguren, J., Galdos, L., Mugarra, E., & de Argandoña, E. S. (2016). Influence of the pressure dependent coefficient of friction on deep drawing springback predictions. *Tribology International*, 103, 266-273.
- [13] Zang, S. L., Lee, M. G., & Kim, J. H. (2013). Evaluating the significance of hardening behavior and unloading modulus under strain reversal in sheet springback prediction. *International Journal of Mechanical Sciences*, 77, 194-204.